JPET Fast Forward. Published on July 19, 2007 as DOI: 10.1124/jpet.107.122119

Title Page

Inhibition of ryanodine receptors by FLA 365 in canine pulmonary arterial smooth muscle cells

Olga Ostrovskaya, Ravi Goyal, Noah Osman, Claire E McAllister, Isaac N Pessah, Joseph R Hume, Sean M Wilson

Department of Pharmacology, University of Mississippi School of Pharmacy and Research Institute of Pharmaceutical Sciences University, MS 38677 (OO, RG, NO, SMW)

University of Mississippi Light Microscopy Core, University, MS 38677 (NO, SMW)

Department of Pharmacology, University of Nevada School of Medicine, Reno, NV 89557 (CEM, JRH)

Department of Molecular Biosciences, School of Veterinary Sciences, University of California, Davis, CA 95616 (INP)

Running Title Page

Running Title: FLA 365 and ryanodine receptors in arterial myocytes

Corresponding Author: Sean M Wilson

University of Mississippi School of pharmacy

University of Mississippi

303 Faser Hall

Phone: 662-915-7255, Fax: 662-915-5148

Email: Wilson@olemiss.edu

Number of text pages : 40

Number of References: 40

Number of tables : 0

Figures : 8

Number of words in the Abstract: 248

Number of words in the Introduction: 595

Number of words in the Discussion: 1428

Nonstandard Abbreviations: PASMC, Rya, RyR, SR, $InsP_3$, $InsP_3R$, CCh, BK, RuR, Ca_V, K_{ATP}, 2-APB.

A recommended section assignment: Cardiovascular

JPET Fast Forward. Published on July 19, 2007 as DOI: 10.1124/jpet.107.122119
This article has not been copyedited and formatted. The final version may differ from this version.

Abstract

Ryanodine is a selective ryanodine receptor (RyR) blocker, with binding dependent on RyR opening. In whole-cell studies, ryanodine binding can lock the RyR in an open-conductance state, short-circuiting the sarcoplasmic reticulum (SR), which restricts studies of $InsP_3$ receptor ($InsP_3R$) activity. Other RyR blockers have non-selective effects that also limit their utility. FLA 365 (4-(2-aminopropyl)-3,5-dichloro-N,N-dimethylaniline, FLA) blocks RyR elicited Ca^{2+} increases in skeletal and cardiac muscle, yet its actions on smooth muscle are unknown. Canine pulmonary arterial smooth muscle cells (PASMCs) express both RyRs and $InsP_3Rs$; thus, we tested the ability of FLA to block RyR and serotonin-mediated $InsP_3R$ elicited Ca^{2+} release by imaging fura-2 loaded PASMCs. Acute exposure to 10 mM caffeine, a selective RyR activator, induced Ca^{2+} increases that were reversibly reduced by FLA with an estimated IC_{50} of ~ 1 - 1.5 μM and inhibited by 10 μM ryanodine or 10 μM cyclopiazonic acid. FLA also blocked L-type Ca^{2+} channel activity, with 10 μM reducing Ba^{2+} current amplitude in patch voltage-clamp studies to 54 ± 6% of control and 100 μM FLA reducing membrane current to 21 ± 6%. $InsP_3R$-mediated Ca^{2+} responses elicited by 10 μM 5-HT in canine PASMCs and 100 μM carbachol in HEK-293 cells were not reduced by 2 μM FLA but were reduced by 20 μM FLA to 76 ± 9% of control in canine PASMCs and 52 ± 1 % in HEK-293 cells. Thus, FLA preferentially blocks RyRs with limited inhibition of L-type Ca^{2+} channels or $InsP_3R$ in canine PASMCs.

Introduction

Ryanodine receptors (RyR) are expressed on the sarcoplasmic reticulum (SR) membranes of excitable cells including smooth muscle myocytes. Opening of these Ca^{2+} permeable channels is predominately dependent on elevations in cytosolic Ca^{2+}, and opening of clusters of RyRs gives rise to Ca^{2+} spark events in many smooth muscle preparations including pulmonary arterial smooth muscle cells (PASMCs) (Janiak, et al., 2001). These Ca^{2+} spark events are particularly important for activation of the large-conductance Ca^{2+} and voltage activated K^+ channel (BK) in vascular smooth muscle (Jaggar, et al., 1998; Zhuge, et al., 2002) and may open Cl^- channels in PASMCs (Janssen and Sims, 1992; Zhuge, et al., 1998). Thus, RyR activity is important to the regulation of pulmonary as well as systemic vascular tone.

The nomenclature of RyRs is due to the fact that the plant alkaloid ryanodine binds with high selectivity to this ion channel. Yet, ryanodine binding is dependent on RyR opening with both concentration and time dependent effects on channel gating. Low ryanodine concentrations or short exposure periods lock the channel into a subconductance state whereas high ryanodine concentrations and long exposure times fully block the channel (Pessah and Zimanyi, 1991). Thus, in whole-cell studies of smooth muscle ryanodine often locks the RyR into an open sub-conductance state, which then leads to depletion of the SR Ca^{2+} stores (Janiak, et al., 2001; Wilson, et al., 2002). Ryanodine-mediated depletion of the SR Ca^{2+} stores then may activate store-operated Ca^{2+} influx pathways, which could influence data interpretation (Wilson, et al., 2002). Given that the

JPET Fast Forward. Published on July 19, 2007 as DOI: 10.1124/jpet.107.122119
This article has not been copyedited and formatted. The final version may differ from this version.

inositol-1,4,5-trisphosphate receptor ($InsP_3R$) may also be on contiguous membrane with RyRs it can be difficult to study the $InsP_3R$ or RyR activation in isolation or potential interactions between the two SR Ca^{2+} release channels. Because of this there is a need for potent RyR antagonists that have little or no effect on other aspects of intracellular Ca^{2+} homeostasis.

A number of compounds are commonly used as RyR channel blockers, but like ryanodine their use can also be problematic. The polycationic dye ruthenium red (RuR) is a well known RyR channel blocker (Chen and MacLennan, 1994; Ma, 1993; Smith, et al., 1988). However, it can block voltage-gated Ca channels (Ca_V) (Cibulsky and Sather, 1999), several transient receptor potential (TRP) channel isoforms (Bleakman, et al., 1990; Dray, et al., 1990;Nagata, et al., 2005), K channels (Hirano, et al., 1998; Lin and Lin-Shiau, 1996; Wann and Richards, 1994), and Ca^{2+}-binding proteins (Charuk, et al., 1990). RuR also alters the Ca^{2+} uptake and release properties of mitochondria (Rossi, et al., 1973). Neomycin affects RyR similarly to RuR but it too blocks Ca_V (Canzoniero, et al., 1993), as well as ATP-activated K channels (K_{ATP}) (Lin, et al., 1993), and phospholipase C (PLC) (Wang, et al., 2005). The anesthetic tetracaine is a well used RyR inhibitor but importantly it inhibits $InsP_3R$ activity (MacMillan, et al., 2005). FLA 365 (4-(2-aminopropyl)-3,5-dichloro-N,N-dimethylaniline) was originally designed as a monamine oxidase (MAO) inhibitor (Ask, et al., 1985; Ask and Ross, 1987). FLA 365 also reduces RyR elicited Ca^{2+} release from the SR of skeletal and cardiac muscle (Calviello and Chiesi, 1989; Chiesi, et al., 1988; Mack, et al., 1992) and inhibits ryanodine binding (Mack, et

JPET Fast Forward. Published on July 19, 2007 as DOI: 10.1124/jpet.107.122119
This article has not been copyedited and formatted. The final version may differ from this version.

al., 1992) and yet the actions of FLA 365 on smooth muscle Ca^{2+} signaling are unknown. Canine PASMCs isolated from pulmonary resistance arteries have well described caffeine-ryanodine and $InsP_3$ sensitive Ca^{2+} release stores (Janiak, et al., 2001), making this an excellent arterial smooth muscle model for pharmaceutical studies involving SR Ca^{2+} metabolism. The present series of experiments take advantage of the SR Ca^{2+} store properties to test the hypothesis that FLA 365 inhibits RyR function in arterial smooth muscle.

Methods

Cell isolation

Smooth muscle cells were isolated from high resistance canine pulmonary arteries as previously described (Janiak, et al., 2001; Wilson, et al., 2002). Mongrel dogs of either sex were sacrificed with pentobarbital sodium (45 mg kg^{-1} I.V.) and ketamine (15 mg kg^{-1} I.V.), as approved by the University of Nevada at Reno Institutional Animal Care and Use Committee. The heart and lungs were excised *en bloc*. The third and fourth branches of pulmonary arteries were dissected at 5^{o} C to decrease cellular metabolic activity. Pulmonary artery isolations and smooth muscle cell dispersions were made in a low-Ca^{2+} physiological saline solution (PSS) containing in mM: 125 NaCl; 5.36 KCl; 0.336 Na_2HPO_4; 0.44 K_2HPO_4; 11 HEPES; 1.2 $MgCl_2$; 0.05 $CaCl_2$; 10 glucose; pH 7.4 (adjusted with Tris), osmolarity 300 mOsm. Arteries were cleaned of connective tissue, cut into small pieces and placed in a tube containing fresh PSS. Tissue was immediately digested or stored at 5^{o} C up to 24 hours. To disperse cells, tissue was placed in low-Ca^{2+} PSS containing enzymes (in mg ml^{-1}): 0.5 collagenase type XI; 0.03 elastase type IV, and 0.5 bovine serum albumin (fat-free) for 14-16 hours at 5^{o} C. In many cases tissues in digestion solution were shipped overnight from the University of Nevada to the University of Mississippi at 5^{o} C. The tissue was then washed several times with 5^{o} C low-Ca^{2+} PSS solution and triturated with a fire-polished Pasteur pipette. The resulting dispersed PASMCs were cold stored at 5^{o} C up to 8 hours until experiments were performed.

Cell culture

HEK 293 cells obtained from ATCC were cultured at 37^{o} C in Eagles modified essential medium (EMEM) containing 10% fetal bovine serum in 5% CO_2. For Ca^{2+} measurements, cells were plated on glass coverslips (Corning Incorporated, NY) and used within 48–72 h after plating.

Fluorescence imaging

The cytosolic [Ca^{2+}] was measured in canine PASMCs or HEK 293 cells loaded with the ratiometric Ca^{2+} sensitive dye fura-2 AM (Molecular Probes, Eugene, OR) using a dual excitation digital Ca^{2+} imaging system (IonOptix Inc., Milton, MA) equipped with an intensified CCD. The imaging system was mounted on a TS100 inverted microscope (Nikon Inc., Melville, NY) outfitted with a 40X (NA 1.3, Nikon) oil immersion objective. Fura-2 AM was dissolved in DMSO and added from a 1 mM stock to the PASM cell suspension or HEK 293 cells attached to coverslips at a final concentration of 10 μM. Cells were loaded with fura-2 AM for 20-30 min in a perfusion chamber (Warner Instruments, Hamden, CT) at room temperature in the dark. Cells were then washed for 30 min to allow for dye esterification at 1 ml min^{-1} with a balanced salt solution of the following composition (mM): 126 NaCl; 5 KCl; 0.3 NaH_2PO_4; 10 HEPES; 1 $MgCl_2$; 2 $CaCl_2$; 10 glucose; pH 7.4 (adjusted with NaOH) 285 - 295 mOsm. Cells were continuously perfused with a peristaltic pump (Rainin, Woburn, MA or Masterflex Cole Parmer, Vernon Hills, IL) and solution flow controlled with a multichannel ValveBank computerized system connected to pinch valves (Automate Scientific,

Berkeley, CA). Measurements of cytosolic [Ca^{2+}] before and during pharmacological manipulation were made once the fura-2 fluorescence ratio stabilized. Cells were illuminated with a xenon arc lamp at 340 and 380 nm (Chroma Technology Corp., Rockingham, VT) and emitted light was collected from regions that encompassed single cells with a CCD at 510 nm. In most experiments, images were acquired at 1 Hz and stored on either compact disk or magnetic media for later analysis. Although it is difficult to precisely measure the intracellular calcium concentration ($[Ca^{2+}]_I$) (Baylor and Hollingworth, 2000) estimates were made from the relation $[Ca^{2+}]_I = K_d * (Sf_2/Sb_2) * (R-R_{min})/(R_{max}-R)$, where R_{min} and R_{max} are the F_{340}/F_{380} ratios of Ca^{2+}-free and Ca^{2+} saturated fura-2 respectively. Sf_2 is the F_{380} of Ca^{2+} free fura-2 and Sb_2 is F_{380} of Ca^{2+} bound fura-2. The values of Sf_2 and R_{min} were determined by bathing cells in a balanced salt solution that did not have any added Ca^{2+} and contained 10 mM EGTA and 1 μM ionomycin. The values of Sb_2 and R_{max} were determined by bathing cells in a balanced salt solution that contained 10 mM Ca^{2+} and 1 μM ionomycin. The K_d for fura-2 was assumed to be 224 nM (Grynkiewicz, et al., 1985). Experimental temperature was 22-25^{o} C.

Electrophysiology

Ba^{2+} currents (I_{Ba}) through L-type Ca^{2+} channels were measured using the dialyzed whole-cell configuration of the patch voltage-clamp technique (Hamill, et al., 1981). The voltage protocol used to record I_{Ba} consisted of a holding potential of -80 mV and cells were depolarized with 100 ms pulses to +10

mV once every 3s. The capacitance was directly read from the HEKA EPC10 amplifier (HEKA Instruments Inc., Southboro, MA) once the cell capacitance was compensated. Micropipettes were pulled from glass capillaries (BF 150-86-10, Sutter Instrument Co, CA) with a Sutter P97 horizontal pipette puller and had tip resistances in the range of 2-5 MΩ**.** Series resistance was compensated 50-80 % if needed in order to give a final value below 10 MΩ. Amplified currents were acquired through a LIH-1600 (HEKA Instruments Inc., Southboro, MA) computer interface card and filtered through 2 filters with the first being 10 KHz and the second 2.9 KHz. Data was acquired with Patchmaster v. 2.1 (HEKA Instruments Inc., Southboro, MA) and stored on magnetic media and compact disk for offline analysis.

Cells were perfused during all experiments with an external solution using a gravity perfusion system at ~1 ml/min and solution flow controlled with a multichannel ValveLink electronically controlled system connected to pinch valves (Automate Scientific, Berkeley, CA). The external solution had the following composition (mM): 118 NaCl; 5 CsCl; 10 Hepes; 1 $MgCl_2$; 10 Glucose; 10 $BaCl_2.2H_2O$, pH=7.4 (adjusted with NaOH), 280 - 290 mOsm. The pipette solution was (mM): 118 CsCl; 10 TEA-Cl; 10 EGTA; 10 Hepes; 0.1 GTP; 5 $ATPNa_2$ and 2 $MgCl_2$, pH=7.3 (adjusted with CsOH), 280 - 290 mOsm as determined with an osmometer (Wescor, Model 5520 Logan UT).

Chemicals and drugs

FLA 365 was provided by I.N. Pessah. Ionomycin free acid ($C_{41}H_{70}O_9$) was purchased from Calbiochem (San Diego, CA), Fura-2 acetoxymethyl ester

JPET Fast Forward. Published on July 19, 2007 as DOI: 10.1124/jpet.107.122119
This article has not been copyedited and formatted. The final version may differ from this version.

(AM) from Invitrogen (Carlsbad, CA) or Molecular Probes (Eugene, OR), 5-HT (serotonin or 5-Hydroxytryptamine), carbachol (2-carbamoyloxyethyl-trimethyl-azanium chloride), ryanodine ($C_{25}H_{35}NO_9$), cyclopiazonic acid ($C_{20}H_{20}N_2O_3$), caffeine (1,3,7-trimethylxanthine), verapamil (2-(3,4-dimethoxyphenyl)-5-[2-(3,4-dimethoxyphenyl)ethyl-methyl-amino]-2-(1-methylethyl) pentanenitrile), nifedipine (dimethyl2,6-dimethyl-4-(2-nitrophenyl)- 1,4-dihydropyridine-3,5-dicarboxylate), and all other chemicals purchased from Sigma (St. Louis, MO).

Statistical analysis

All data are presented as mean ± S.E.M. Statistical difference within cell groups was determined with a two-tailed paired Student's *t* test. Statistical tests between groups were performed with analysis of variance (ANOVA) with the specific test being chosen dependent on the type of samples being examined, normality of the dataset or the variability within or between groups. A Kruskal-Wallis One-way ANOVA on Ranks with a Dunns Pairwise Multiple Comparison Procedure was used if the data distribution did not pass normality. A One-way ANOVA with a Newman-Keuls or a Bonforroni's Multiple Comparison Test was used for comparing different independent cell groups. A Repeated measures ANOVA with a Newman-Keuls Multiple Comparison Test was used to test the difference between the effects of different conditions in the same cell group. The specific test used for each data set is noted in the legend for each figure. A *P* value < 0.05 was accepted as statistically significant. The n values reported reflect the total number of cells tested. For the dose response curve depicted in figure 1B the following number of cells were examined and treated with the

following concentrations of FLA 365; 20 cells were not exposed to FLA 365, 9 cells were treated with 1 nM, 20 with 10 nM, 14 with 1 μM, 21 with 2 μM, 11 with 10 μM, 24 with 20 μM, 7 with 50 μM and 11 with 200 μM. Multiple trials were performed on cells isolated from multiple dogs for most experimental paradigms. When HEK 293 cells were used, at least 3 independent experimental runs were performed.

A Hill equation of the form $R/R_{control} = A_1 + (A_2 – A_1) / (1+10^((logxo-x)*p))$ was used to determine the half-maximum inhibition and hillslope of caffeine mediated Ca^{2+} increases by FLA 365, where A_1 = bottom asymptote, A_2 = top asymptote, Log xo = IC_{50}, p = hill slope, R is $\Delta F_{340}/F_{380}$ to caffeine in the presence of varied concentrations of FLA 365 while $R_{control}$ is $\Delta F_{340}/F_{380}$ in the absence of FLA 365.

JPET Fast Forward. Published on July 19, 2007 as DOI: 10.1124/jpet.107.122119
This article has not been copyedited and formatted. The final version may differ from this version.

Results

FLA 365 causes a reversible inhibition of RyR in canine PASMCs.

Canine PASMC have caffeine-ryanodine and $InsP_3$ sensitive SR Ca^{2+} stores (Janiak, et al., 2001), which makes them an excellent model system for pharmacological examinations of compounds that may effect RyR or $InsP_3R$ activity. Figure 1A shows the Ca^{2+} response to 10 mM caffeine in an individual canine PASMC and the blocking action of two concentrations of FLA 365. Exposure of the cell to 2 μM FLA 365 did not alter the cytosolic Ca^{2+} concentration on its own, but reduced the Ca^{2+} response to 10 mM caffeine by ~ 75%. Elevating FLA 365 to 200 μM induced a transient increase in the cytosolic Ca^{2+} concentration. Cells treated with FLA 365 concentrations ≥ 20 μM also had Ca^{2+} elevations and are presented in Figure 4. Exposure to 10 mM caffeine in the continued presence of 200 μM FLA 365 did not cause any cytosolic Ca^{2+} increase.

A more detailed analysis of the potency of FLA 365 to inhibit caffeine elicited Ca^{2+} release events in PASMCs was then performed. Figure 1B illustrates that FLA 365 inhibits the caffeine release events in a concentration dependent manner, though at concentrations > 2 μM the compound may have limited usefulness as indicated by the reduced potency at 20 μM. Because of the potential for the 20 μM value being an outlier or due to non-selective actions of FLA 365 on Ca^{2+} metabolism two dose-response curves were fit to the data including (dashed line) and excluding (solid line) 20 μM FLA 365. The estimated IC_{50} exclusive of 20 μM FLA 365 had a 95 % confidence interval of 1 to 1.5 μM

and 1.3 to 3.5 μM inclusive of the data point, with respective mean values of 1.24 and 2.3 μM, and Hill coefficients of -0.44 and -0.31. Notably the R^2 value for the curve fit was 0.97 exclusive of the 20 μM FLA 365 value, which was substantially higher than 0.84 when the data point was included. The calculated IC_{50} exclusive of the 20 μM data value is roughly one-half the previously established value in skeletal and cardiac SR vesicles of 3 μM (Calviello and Chiesi, 1989), suggesting there may be differences in the ability of FLA 365 to inhibit RyR expressed in smooth muscle relative to that in skeletal or cardiac muscle. Given that the Hill coefficient was also substantially lower than 1 there may be non-cooperative binding of two or more FLA 365 molecules on each RyR.

For comparative purposes and to show some of the potential utility of FLA 365 a series of experiments were performed where 10 μM ryanodine or 10 μM cyclopiazonic acid, a sarcoplasmic-endoplasmic reticulum Ca^{2+} ATPase (SERCA) inhibitor, were used to inhibit caffeine-elicited RyR mediated Ca^{2+} responses. Figure 2A shows that 10 mM caffeine applications repeated every 3 minutes elicited Ca^{2+} responses of similar magnitude in an individual canine PASMC. Figure 2B then shows an individual myocyte exposed to 10 μM ryanodine, where the Ca^{2+} response to 10 mM caffeine decayed with sequential stimulations. Figure 2C shows that 10 μM cyclopiazonic acid induced Ca^{2+} elevations on its own, corresponding to SERCA inhibition and passive loss of Ca^{2+} from the SR. Cyclopiazonic acid also reduced and ablated the responses to 10 mM caffeine through the loss of stored Ca^{2+}. Figure 2D summarizes the changes in the magnitude of the Ca^{2+} release events with repeated caffeine

applications in the absence and presence of 10 μM ryanodine or 10 μM cyclopiazonic acid. The figure illustrates that the Ca^{2+} response to 10 mM caffeine is reduced in the presence of ryanodine, with the 2nd caffeine response being 73 ± 11 % of the control and 34 ± 5 % with a 3rd caffeine treatment. Cyclopiazonic acid similarly reduced the Ca^{2+} elevations due to caffeine, where the 2nd caffeine response was 27 ± 3 % of the control and 2 ± 1 % when treated with caffeine once more. These ryanodine and cyclopiazonic acid dependent decrements in Ca^{2+} responsiveness to caffeine are similar to the results that we have previously published (Janiak, et al., 2001; Wilson, et al., 2002). Comparatively, in cells that were not treated with ryanodine or cyclopiazonic acid there were not any decreases in the Ca^{2+} responses to sequential applications of caffeine. The 2nd caffeine application elicited a Ca^{2+} response that was 119 ± 8% of the first caffeine exposure (i.e. control) while a third application was 142 ± 8%.

The reversibility of FLA 365 was then examined to further evaluate the compounds properties. Figure 3A shows the Ca^{2+} response to 10 mM caffeine in an individual canine PASMC and the reversible nature of the inhibitory actions of 20 μM FLA 365 on the Ca^{2+} release event. This concentration was chosen as it is well above the IC_{50} required for FLA 365 to inhibit ryanodine binding to the RyR in skeletal muscle microsomal preparations (Mack, et al., 1992). Figure 3B summarizes these release events and shows that before FLA 365 the Ca^{2+} response to caffeine was 160 ± 18 nM. Brief exposure to 20 μM FLA 365 decreased the Ca^{2+} release due to 10 mM caffeine to 47 ± 7 nM. Removal of FLA

365 from the bathing solution allowed for full restoration of the Ca^{2+} response to caffeine, which was 155 ± 15 nM.

FLA 365 is known to cause rapid inhibition of RyR activity (Calviello and Chiesi, 1989; Chiesi, et al., 1988; Mack, et al., 1992), though there may be a short latency between FLA 365 binding and RyR block. During this time the RyR may be in a longer-lived open state, which would allow for significant Ca^{2+} flux, such as occurs with ryanodine binding. To test this we examined the actions of FLA 365 on resting myocytes. Figure 4A shows a representative cell where 20 μM FLA 365 did cause a significant increase in the cytosolic [Ca^{2+}]. Figure 4B summarizes the Ca^{2+} responses for the FLA 365-responsive myocytes, illustrating that 20 μM FLA 365 caused the cytosolic [Ca^{2+}] to rise 100 nM, from 128 ± 19 nM to 228 ± 25 nM in the 8 cells where FLA 365 induced Ca^{2+} increases. Figure 4C illustrates that Ca^{2+} elevations due to 20 μM FLA 365 are infrequent, occurring in only 8 of 48 myocytes (16.7%). Notably cells exposed to > 20 μM FLA 365 also had cytosolic Ca^{2+} increases as illustrated for 200 μM FLA 365 in Figure 1A whereas those exposed to 2 μM or lower concentrations did not.

FLA 365 blocks L-type Ca channels in PASMCs.

FLA 365 is a phenylalkylamine, and thus belongs to the same major chemical class as verapamil, which is a potent and selective blocker of L-type Ca^{2+} channels (Catterall, et al., 2005). Because of this we tested the hypothesis that FLA 365 would reduce Ca_V function in PASMCs. To assess the function of Ca_V, Ba^{2+} currents were measured using whole-cell patch voltage clamp techniques (del Corsso, et al., 2006). Figure 5A shows the percentage of the

peak Ba^{2+} current in an individual myocyte held at -80 mV and stepped to +10 mV every 3 seconds, which elicits Ca_V activity. In this cell there was very little run-down of the current amplitude over time and on average there was only a modest run-down of the membrane current, being 92 ± 3 % of the initial value (Fig. 5D). Figure 5B shows that 10 μM verapamil caused the Ba^{2+} current to be reduced to ~ 25% of the initial amplitude. On average, 10 μM verapamil caused the Ba^{2+} current amplitude to be reduced to 15 ± 6%. The effects of FLA 365 on voltage-activated Ba^{2+} currents were then examined at 10 and 100 μM, which are well above the IC_{50} for FLA 365 inhibition of the RyR. Figure 5C illustrates that 100 μM FLA 365 caused a reduction in the Ba^{2+} current amplitude, which is comparable to that of 10 μM verapamil. Figure 5D shows that on average Ba^{2+} currents were reduced to 54 ± 6% of the control current by 10 μM FLA 365, while 100 μM FLA 365 reduced the current to 21 ± 6% compared to control. Thus, FLA 365 exerts a significant block on I_{Ba} in canine PASMC with an approximated IC_{50} of 10 μM, which is about one order of magnitude higher than the IC_{50} of RyR block by FLA 365 (Figure 1).

A series of Ca^{2+} imaging experiments were performed to evaluate Ca_V activity during caffeine and 5-HT exposure because 20 μM FLA 365 may inhibit Ca_V responses and thereby reduce the peak Ca^{2+} response during cell stimulation. Figure 6A shows that in an individual canine PASMC there was not any reduction in the peak Ca^{2+} response with repeated exposure to 10 mM caffeine. Figure 6B shows a myocyte where 10 μM verapamil failed to diminish the Ca^{2+} response to 10 mM caffeine Figure 6C shows that 10 μM nifedipine did

not reduce 10 μM 5-HT elicited Ca^{2+} elevations in an individual canine PASMC and that Ca^{2+} responsiveness is maintained with repeated 5-HT exposures.

Figure 6D summarizes the data showing the percentage change in the peak height of the F_{340}/F_{380} response when comparisons are made between responses to two sequential caffeine applications in the absence of antagonists (i.e. control) or absence and then presence of 20 μM FLA 365, 10 μM verapamil or 10 μM nifedipine. The figure illustrates that 20 μM FLA 365 but not 10 μM verapamil or 10 μM nifedipine cause significant reductions in the Ca^{2+} response to 10 mM caffeine. The Ca^{2+} response to caffeine was 85 ± 4% in time matched controls, 87 ± 9 % of its control in the presence of nifedipine and 89 ± 3 % in cells exposed to verapamil. In comparison, the Ca^{2+} response to caffeine in the presence of 20 μM FLA 365 was 41 ± 7 %. In addition, Figure 6D shows that Ca^{2+} responses to 10 μM 5-HT were also unaffected by nifedipine, being 96 ± 14 % of their respective controls.

FLA 365 reduces 5-HT mediated Ca^{2+} responses in canine PASMCs.

Even though FLA 365 has long been known to inhibit RyR activity, its actions on $InsP_3$ related Ca^{2+} release events have not been previously examined. This question was explored by testing the actions of FLA 365 on 5-HT elicited Ca^{2+} responses in canine PASMCs. The 5-HT Ca^{2+} responses in canine pulmonary arterial myocytes are due to the activity of $InsP_3$ receptors as the responses are blocked by ketanserin, a selective 5-HT_{2A} receptor antagonist as well as by the $InsP_3$ receptor blockers 2-aminobiphenylborate (2-APB) and xestospongin C (Wilson, et al., 2005). Figure 7A as well as Figure 6C show that

5-HT exposures repeated ~ 5 minutes can induce Ca^{2+} responses of similar magnitude. Figure 7B shows that when treated with 2 μM FLA 365 the amplitude of the 5-HT elicited Ca^{2+} response is unaffected while 10 mM caffeine elicited Ca^{2+} responses are significantly depressed. Figure 7C illustrates that 20 μM FLA 365 reduces the amplitude of the 5-HT elicited Ca^{2+} response by ~25% and reduces 10 mM caffeine elicited Ca^{2+} increases substantially more.

Figure 7D summarizes data showing the percentage change in the peak height of the F_{340}/F_{380} response when comparisons are made between cells exposed twice to 10 μM 5-HT in the absence of antagonists (i.e. control, Figure 7A) or absence and then presence of 2 μM or 20 μM FLA 365. The figure illustrates that 20 μM but not 2 μM FLA 365 reduces the amplitude of the Ca^{2+} responses due to 10 μM 5-HT in canine PASMCs. The Ca^{2+} response to 10 μM 5-HT was 91 ± 5 % of the initial 5-HT response in cells that were not treated with any antagonists, 104 ± 5 % in presence of 2 μM FLA 365, and 76 ± 9 % in the presence of 20 μM FLA 365. Figure 7D also shows comparative effects on caffeine induced Ca^{2+} responses in those cells treated with 2 μM FLA 365, where the Ca^{2+} increase to 10 mM caffeine was substantially reduced, being 25 ± 4 % of control.

The potential for complex interactions between $InsP_3$ and RyR Ca^{2+} signaling in vascular myocytes has the potential to lead to misinterpretation of the preceding findings. A series of experiments to verify that FLA 365 can block $InsP_3$ receptor-mediated responses was therefore conducted in HEK 293 cells, which express predominantly $InsP_3$ receptors. Although RyRs may be expressed

in HEK 293 cells in early passages (Luo, et al., 2005) the cells examined did not exhibit Ca^{2+} responses to 10 mM caffeine (data not shown). To further limit possible RyR contamination, caffeine was applied in every experiment to ensure that cells expressed $InsP_3$ receptors but not RyRs. Figures 8A and B show representative traces of $InsP_3$ receptor-mediated responses elicited with 100 µM CCh in the absence and presence of 2 µM or 20 µM FLA 365. Figure 8C summarizes the data showing 20 µM FLA 365 inhibited CCh mediated Ca^{2+} elevations by 52 ± 1 %. Yet, 2 µM FLA 365, which substantially inhibits RyR mediated Ca^{2+} responses in PASMCs (Figures 1 and 7), did not reduce Ca^{2+} responses to CCh (107 ± 3 % of control). Figure 8D illustrates that washing cells exposed to 20 µM FLA 365 allowed for full recovery of the Ca^{2+} response to CCh, being 99 ± 4 % of the control response. Thus, increasing the FLA 365 concentration by an order of magnitude above that needed to reduce RyR activity reversibly inhibits $InsP_3$ receptor activation.

Discussion

In this work we describe for the first time the impact of FLA 365 on Ca^{2+} signaling in smooth muscle, which blocks Ca^{2+} release from the SR of skeletal and cardiac muscle (Calviello and Chiesi, 1989; Chiesi, et al., 1988; Mack, et al., 1992). Our data illustrate that FLA 365 inhibits Ca^{2+} responses due to caffeine in canine PASMCs, indicating that FLA 365 inhibits RyR responses in smooth muscle as well as RyR expressed in other cell types (Janiak, et al., 2001; Wilson, et al., 2002). What is more, the data also provide evidence that FLA 365 can inhibit Ca_V and $InsP_3$ induced Ca^{2+} responses at concentrations higher than that required to inhibit RyR.

FLA 365 has a number of characteristics that are significant to its general utility. FLA 365 inhibition of RyR is readily reversible, and exhibits some selectivity for RyR over inhibition of Ca_V and $InsP_3$ receptors. Low micromolar FLA 365 concentrations significantly reduce, but do not eliminate, RyR activation without effect on $InsP_3$ related responses. FLA 365 at high concentrations blocks Ca_V in canine PASMCs and 5-HT and CCh generated Ca^{2+} release in either canine PASMCs or HEK 293 cells. Although this latter effect of FLA 365 on receptor-mediated Ca^{2+} responses is presumed to be through inhibition of $InsP_3$ receptors the experimental design does not delineate whether FLA 365 may alter ligand-activation of 5-HT or muscarinic receptors or generation of $InsP_3$ by phospholipase C. The differences in potency toward RyR as compared to Ca_V and $InsP_3$ – generated Ca^{2+} responses indicates this compound may have untoward actions on other Ca^{2+} permeable channels. What is more, the data

suggests that FLA 365 may inhibit $InsP_3$ responses more effectively in HEK 293 cells than in canine pulmonary arterial myocytes. The IC_{50} for RyR inhibition in canine PASMCs is also somewhat dissimilar from that in skeletal and cardiac muscle (Calviello and Chiesi, 1989; Chiesi, et al., 1988; Mack, et al., 1992). These findings show that attention should be given to the selectivity as well as potency when FLA 365 is used to study RyR function.

The pharmacological properties of FLA 365 differ from other RyR antagonists and agents used to deplete Ca^{2+} stored in the SR. Ryanodine is time, dose and use dependent, which limits its utility in live-cell studies. This is evidenced by depression of $InsP_3R$ mediated responses due to leak of Ca^{2+} from the SR through RyRs locked in an open sub-conductance state. Tetracaine and dantrolene are similar to FLA 365 in that they too may block $InsP_3$ responses independent of the involvement of RyRs, while neomycin shares inhibition of Ca_V channels (Canzoniero, et al., 1993; Fellner and Arendshorst, 2005; Lin, et al., 1993; Wang, et al., 2005). Cyclopiazonic acid and thapsigargin are two routinely used SERCA inhibitors that passively deplete the SR Ca^{2+} stores (Janiak, et al., 2001; Wilson, et al., 2002). This passive depletion can activate capacitative Ca^{2+} entry and reduce both $InsP_3$ and RyR related Ca^{2+} responses (Janiak, et al., 2001; Wilson, et al., 2002). Sarcoplasmic reticulum Ca^{2+} store depletion therefore would confound selective examination of $InsP_3R$ or RyR activity as well as studies regarding the coupling between Ca^{2+} permeable channels.

Coupling of RyRs to $InsP_3$ receptors are important to smooth muscle function, but yet the extent of these interactions and their functions are poorly

understood. Angiotensin II activates both $InsP_3$ as well as RyR pathways in rat renal arteries (Fellner and Arendshorst, 2005) and RyRs are important during norepinephrine induced contractility and Ca^{2+} signaling in rat pulmonary arteries and myocytes (Zheng, et al., 2005). Zheng *et. al.*, 2005 used a variety of RyR antagonists including dantrolene, tetracaine, RuR as well as ryanodine to evaluate the role of RyR activity during norepinephrine induced Ca^{2+} responses and arterial contractility. FLA 365 would be useful in studies such as these as it is readily reversible and exhibits some selectivity for RyRs over $InsP_3$ receptors.

The experiments presented here do not provide any conclusive evidence for or against possible interactions between RyR and $InsP_3R$ in canine PASMCs. However, our previous work suggests there is little direct activation of RyR during $InsP_3R$ activity in these cells as the RyR Ca^{2+} stores can be depleted without impacting angiotensin II induced, $InsP_3$ related Ca^{2+} release (Janiak, et al., 2001). However, there may be species related differences as Zheng *et.al.* 2005 provide evidence for interactions between $InsP_3$-related and RyR mediated Ca^{2+} responses and functionality in rat pulmonary arteries and myocytes. The functional organization of the RyR and $InsP_3$ Ca^{2+} release pathways would likely be important to arterial reactivity during neuro-humoral stimulation and FLA 365 may be a useful reagent when assessing the organization of these pathways.

The coupling of Ca_V stimulation to RyR activation has also been evaluated in smooth muscle with RyRs underlying Ca^{2+} spark events evoked in response to membrane depolarization and Ca_V activation (Collier, et al., 2000). Ryanodine was used in these real-time laser scanning confocal microscopy experiments to

demonstrate the role of RyR to the Ca^{2+} spark events; FLA 365 would have advantages in these types of studies as it is rapidly acting and reversible. In particular, our studies indicate low concentrations of FLA 365 would reduce RyR activity, allowing for spatial and temporal examinations of RyR coupling to other Ca^{2+} permeable channels such as Ca_V and $InsP_3$ receptors. Secondarily, the preparation should recover following compound washout allowing for additional evaluations in the same preparation.

The mechanism of FLA 365 inhibition of the RyR is important to its usefulness. In particular, kinetic Ca^{2+} uptake and release studies performed on skeletal and cardiac SR vesicles showed that FLA 365 inhibited Ca^{2+} release monophasically with an IC_{50} of 3.4 μM (Calviello and Chiesi, 1989). The action of FLA 365 was synergistic with neomycin and ruthenium red in skeletal and cardiac SR vesicles (Calviello and Chiesi, 1989; Chiesi, et al., 1988). Mack *et.al.* 1992 provided evidence of multiple binding sites for FLA 365 in the same preparation, where FLA 365 could compete for occupation of one of the RyR binding sites while neomycin or ruthenium red would occupy the other (Mack, et al., 1992). Our data suggests that as many as two FLA 365 molecules may be required to inhibit the RyR in canine PASMC, signifying that the actions of FLA 365 may be complex.

FLA 365 is an important RyR inhibitor in that it does not allow for long-lived RyR channel openings, which contrasts the effects of ryanodine. It has previously been suggested that FLA 365 may act as an open channel inhibitor, where the FLA may bind when the RyR is activated and there is maximal Ca^{2+}

efflux rate. Yet, FLA 365 does not induce the subconductance states that underlie the long-lived RyR channel openings (Calviello and Chiesi, 1989; Mack, et al., 1992). Our data suggest that FLA 365 is not likely to cause these long-lived channel openings in smooth muscle myocytes because short incubations were sufficient to reduce caffeine elicited Ca^{2+} responses. What is more, the slow Ca^{2+} rise generally afforded with ryanodine (e.g. Figure 2B) was not observed in most cells.

FLA 365 concentrations > 20 μM induced small amplitude Ca^{2+} transients that may be due to short-lived RyR channel openings that occur before FLA 365 can bind fully and completely block channel activity. Even still, this phenomenon was not observed at ≤ 2 μM FLA 365, concentrations that would be more typically used to antagonize RyR activity.

The data presented provide evidence that Ca_V does not contribute significantly to the peak height of Ca^{2+} release due to caffeine or 5-HT in canine pulmonary myocytes. Our recently published work indicates that 5-HT elicited Ca^{2+} increases were not markedly affected when Ca_V was inhibited (Wilson, et al., 2005). In this same report Ca_V is shown to be important to sustained 5-HT mediated Ca^{2+} responses and arterial contractility, which is common among other G-protein coupled pathways in arteries (Wilson, et al., 2005). The present studies do, however, provide further support for the premise that transient Ca^{2+} responses due to RyR or $InsP_3$ receptor activation do not significantly recruit Ca_V Ca^{2+} entry pathways in canine PASMCs.

Overall, the studies offer evidence that FLA 365 inhibits RyRs in smooth muscle. Albeit, further investigations could be performed to assess potential limitations due to inhibition of other mechanisms of Ca^{2+} signaling, such as the mitochondrial uniporter, which may be a RyR (Beutner, et al., 2001; Beutner, et al., 2005) or non-selective cation channels. Even though FLA 365 has a narrow selectivity window and it does not fully inhibit RyRs its rapid reversibility and distinctive properties may provide researchers a useful pharmacological tool to examine intracellular Ca^{2+} signaling dynamics in vascular smooth muscle and other preparations.

Acknowledgments

We would like to thank Matthew Loftin, Will Graugnard, Phillip Keller and Shen Xiao-Ming for technical assistance.

References

Ask AL, Fagervall I, Florvall L, Ross SB and Ytterborn S (1985) Inhibition of monoamine oxidase in 5-hydroxytryptaminergic neurones by substituted p-aminophenylalkylamines. *Br J Pharmacol* **85**:683-690.

Ask AL and Ross SB (1987) Inhibition of 5-hydroxytryptamine accumulation and deamination by substituted phenylalkylamines in hypothalamic synaptosomes from normal and reserpine-pretreated rats. *Naunyn Schmiedebergs Arch Pharmacol* **336**:591-596.

Baylor SM and Hollingworth S (2000) Measurement and Interpretation of Cytoplasmic [Ca2+] Signals From Calcium-Indicator Dyes. *News Physiol Sci* **15**:19-26.

Beutner G, Sharma VK, Giovannucci DR, Yule DI and Sheu SS (2001) Identification of a ryanodine receptor in rat heart mitochondria. *J Biol Chem* **276**:21482-21488.

Beutner G, Sharma VK, Lin L, Ryu SY, Dirksen RT and Sheu SS (2005) Type 1 ryanodine receptor in cardiac mitochondria: transducer of excitation-metabolism coupling. *Biochim Biophys Acta* **1717**:1-10.

Bleakman D, Brorson JR and Miller RJ (1990) The effect of capsaicin on voltage-gated calcium currents and calcium signals in cultured dorsal root ganglion cells. *Br J Pharmacol* **101**:423-431.

Calviello G and Chiesi M (1989) Rapid kinetic analysis of the calcium-release channels of skeletal muscle sarcoplasmic reticulum: the effect of inhibitors. *Biochemistry* **28**:1301-1306.

Canzoniero LM, Taglialatela M, Di Renzo G and Annunziato L (1993) Gadolinium and neomycin block voltage-sensitive Ca2+ channels without interfering with the Na(+)-Ca2+ antiporter in brain nerve endings. *Eur J Pharmacol* **245**:97-103.

Catterall WA, Perez-Reyes E, Snutch TP and Striessnig J (2005) International Union of Pharmacology. XLVIII. Nomenclature and structure-function relationships of voltage-gated calcium channels. *Pharmacol Rev* **57**:411-425.

Charuk JH, Pirraglia CA and Reithmeier RA (1990) Interaction of ruthenium red with Ca2(+)-binding proteins. *Anal Biochem* **188**:123-131.

Chen SR and MacLennan DH (1994) Identification of calmodulin-, Ca(2+)-, and ruthenium red-binding domains in the Ca2+ release channel (ryanodine receptor) of rabbit skeletal muscle sarcoplasmic reticulum. *J Biol Chem* **269**:22698-22704.

Chiesi M, Schwaller R and Calviello G (1988) Inhibition of rapid Ca-release from isolated skeletal and cardiac sarcoplasmic reticulum (SR) membranes. *Biochem Biophys Res Commun* **154**:1-8.

Cibulsky SM and Sather WA (1999) Block by ruthenium red of cloned neuronal voltage-gated calcium channels. *J Pharmacol Exp Ther* **289**:1447-1453.

Collier ML, Ji G, Wang Y and Kotlikoff MI (2000) Calcium-induced calcium release in smooth muscle: loose coupling between the action potential and calcium release. *J Gen Physiol* **115**:653-662.

del Corsso C, Ostrovskaya O, McAllister CE, Murray K, Hatton WJ, Gurney AM, Spencer NJ and Wilson SM (2006) Effects of aging on Ca2+ signaling in murine mesenteric arterial smooth muscle cells. *Mech Ageing Dev* **127**:315-323.

Dray A, Forbes CA and Burgess GM (1990) Ruthenium red blocks the capsaicin-induced increase in intracellular calcium and activation of membrane currents in sensory neurones as well as the activation of peripheral nociceptors in vitro. *Neurosci Lett* **110**:52-59.

Fellner SK and Arendshorst WJ (2005) Angiotensin II Ca2+ signaling in rat afferent arterioles: stimulation of cyclic ADP ribose and IP3 pathways. *Am J Physiol Renal Physiol* **288**:F785-F791.

Grynkiewicz G, Poenie M and Tsien RY (1985) A new generation of Ca2+ indicators with greatly improved fluorescence properties. *J Biol Chem* **260**:3440-3450.

Hamill OP, Marty A, Neher E, Sakmann B and Sigworth FJ (1981) Improved patch-clamp techniques for high-resolution current recording from cells and cell-free membrane patches. *Pflugers Arch* **391**:85-100.

Hirano M, Imaizumi Y, Muraki K, Yamada A and Watanabe M (1998) Effects of ruthenium red on membrane ionic currents in urinary bladder smooth muscle cells of the guinea-pig. *Pflugers Arch* **435**:645-653.

Jaggar JH, Wellman GC, Heppner TJ, Porter VA, Perez GJ, Gollasch M, Kleppisch T, Rubart M, Stevenson AS, Lederer WJ, Knot HJ, Bonev AD and Nelson MT (1998) Ca2+ channels, ryanodine receptors and Ca(2+)-activated K+ channels: a functional unit for regulating arterial tone. *Acta Physiol Scand* **164**:577-587.

Janiak R, Wilson SM, Montague S and Hume JR (2001) Heterogeneity of calcium stores and elementary release events in canine pulmonary arterial smooth muscle cells. *Am J Physiol Cell Physiol* **280**:C22-C33.

Janssen LJ and Sims SM (1992) Acetylcholine activates non-selective cation and chloride conductances in canine and guinea-pig tracheal myocytes. *J Physiol* **453**:197-218.

Lin MJ and Lin-Shiau SY (1996) Ruthenium red, a novel enhancer of K+ currents at mouse motor nerve terminals. *Neuropharmacology* **35**:615-623.

Lin X, Hume RI and Nuttall AL (1993) Voltage-dependent block by neomycin of the ATP-induced whole cell current of guinea-pig outer hair cells. *J Neurophysiol* **70**:1593-1605.

Luo D, Sun H, Xiao RP and Han Q (2005) Caffeine induced Ca2+ release and capacitative Ca2+ entry in human embryonic kidney (HEK293) cells. *Eur J Pharmacol* **509**:109-115.

Ma J (1993) Block by ruthenium red of the ryanodine-activated calcium release channel of skeletal muscle. *J Gen Physiol* **102**:1031-1056.

Mack WM, Zimanyi I and Pessah IN (1992) Discrimination of multiple binding sites for antagonists of the calcium release channel complex of skeletal and cardiac sarcoplasmic reticulum. *J Pharmacol Exp Ther* **262**:1028-1037.

MacMillan D, Chalmers S, Muir TC and McCarron JG (2005) IP3-mediated Ca2+ increases do not involve the ryanodine receptor, but ryanodine receptor

antagonists reduce IP3-mediated Ca2+ increases in guinea-pig colonic smooth muscle cells. *J Physiol* **569**:533-544.

Nagata K, Duggan A, Kumar G and Garcia-Anoveros J (2005) Nociceptor and hair cell transducer properties of TRPA1, a channel for pain and hearing. *J Neurosci* **25**:4052-4061.

Pessah IN and Zimanyi I (1991) Characterization of multiple [3H]ryanodine binding sites on the Ca2+ release channel of sarcoplasmic reticulum from skeletal and cardiac muscle: evidence for a sequential mechanism in ryanodine action. *Mol Pharmacol* **39**:679-689.

Rossi CS, Vasington FD and Carafoli E (1973) The effect of ruthenium red on the uptake and release of Ca 2+ by mitochondria. *Biochem Biophys Res Commun* **50**:846-852.

Smith JS, Imagawa T, Ma J, Fill M, Campbell KP and Coronado R (1988) Purified ryanodine receptor from rabbit skeletal muscle is the calcium-release channel of sarcoplasmic reticulum. *J Gen Physiol* **92**:1-26.

Wang C, Du XN, Jia QZ and Zhang HL (2005) Binding of PLCdelta1PH-GFP to PtdIns(4,5)P2 prevents inhibition of phospholipase C-mediated hydrolysis of PtdIns(4,5)P2 by neomycin. *Acta Pharmacol Sin* **26**:1485-1491.

Wann KT and Richards CD (1994) Properties of single calcium-activated potassium channels of large conductance in rat hippocampal neurons in culture. *Eur J Neurosci* **6**:607-617.

Wilson SM, Mason HS, Ng LC, Montague S, Johnston L, Nicholson N, Mansfield S and Hume JR (2005) Role of basal extracellular Ca2+ entry during 5-HT-induced vasoconstriction of canine pulmonary arteries. *Br J Pharmacol* **144**:252-264.

Wilson SM, Mason HS, Smith GD, Nicholson N, Johnston L, Janiak R and Hume JR (2002) Comparative capacitative calcium entry mechanisms in canine pulmonary and renal arterial smooth muscle cells. *J Physiol* **543**:917-931.

Zheng YM, Wang QS, Rathore R, Zhang WH, Mazurkiewicz JE, Sorrentino V, Singer HA, Kotlikoff MI and Wang YX (2005) Type-3 ryanodine receptors mediate hypoxia-, but not neurotransmitter-induced calcium release and contraction in pulmonary artery smooth muscle cells. *J Gen Physiol* **125**:427-440.

Zhuge R, Fogarty KE, Tuft RA and Walsh JV, Jr. (2002) Spontaneous transient outward currents arise from microdomains where BK channels are exposed to a mean Ca(2+) concentration on the order of 10 microM during a Ca(2+) spark. *J Gen Physiol* **120**:15-27.

Zhuge R, Sims SM, Tuft RA, Fogarty KE and Walsh JV, Jr. (1998) Ca2+ sparks activate K+ and Cl- channels, resulting in spontaneous transient currents in guinea-pig tracheal myocytes. *J Physiol* **513**:711-718.

Footnotes

This work was supported by NIH grants HL49254 and P20RR15518 from NCRR (JRH), ES11269 and AR17605 (INP), HL10476, AI55462, UM faculty fellowship and a portion of this material is based upon work supported by the National Science Foundation under Grant No. MRI 0619774 (SMW) and UM graduate student fellowship to RG. Present address for Dr. Ostrovskaya is the Department of Pharmacology University of Tennessee, Memphis.

Legends for Figures

Figure 1. FLA 365 causes a concentration dependent inhibition of caffeine elicited cytosolic Ca^{2+} increases in canine PASMCs. (A) Representative tracing of caffeine (CAF) induced Ca^{2+} increases in the absence and presence of 2 μM and then 200 μM FLA 365, (B) Average change in the $\Delta F_{340}/F_{380}$ response to caffeine compared to their respective control values for varied FLA 365 concentrations. Data were fit with a Hill equation exclusive (solid line) or inclusive (dashed line) of 20 μM FLA 365 (open circle). Error bars represent ± SEM.

Figure 2. Ryanodine or cyclopiazonic acid inhibit caffeine elicited cytosolic Ca^{2+} increases in canine PASMCs. Representative tracings of repetitive caffeine induced Ca^{2+} increases in the absence (A) and presence (B) of ryanodine (Rya) or (C) cyclopiazonic acid (CPA). (D) Bars indicate the percentage of the $\Delta F_{340}/F_{380}$ for 10 mM caffeine for the 2nd and 3rd caffeine exposure compared to the first exposure in the absence (solid) or presence of 10 μM Rya (open) or 10 μM CPA (diagonal lines). Significant differences between the responses in the presence and absence of Rya or CPA are denoted for the second and third caffeine applications * ($P<0.05$) and *** ($P<0.001$) by a Kruskal-Wallis One Way Analysis of Variance on Ranks with a Dunns Pairwise Multiple Comparison Procedure. Number in parentheses is the number of cells examined. Error bars represent ± SEM.

Figure 3. FLA 365 reversibly inhibits caffeine elicited cytosolic Ca^{2+} increases in canine PASMCs. (A) Representative tracing of caffeine induced Ca^{2+} increases

in the absence, presence and following washout of 20 μM FLA 365. (B) Bars show the change in cytosolic [Ca^{2+}] from the resting [Ca^{2+}] due to 10 mM caffeine in the absence, presence and following washout of 20 μM FLA 365. * denotes significantly different by Kruskal-Wallis One Way Analysis of Variance on Ranks with a Dunns Pairwise Multiple Comparison Procedure from CAF and CAF (Wash) groups ($P<0.05$). Number in parentheses is the number of cells examined. Error bars represent ± SEM.

Figure 4. FLA 365 elicits cytosolic Ca^{2+} elevations in some canine PASMCs. (A) Effect of 20 μM FLA 365 on the cytosolic [Ca^{2+}] in a responsive cell. (B) Bars show the cytosolic [Ca^{2+}] in the absence and then presence of 20 μM FLA 365. ** denotes significant difference from control by a two-tailed paired t-test ($P<0.01$). (C) Bars show the percentage of cells with (responders, open bars) or without (non-responders, solid bars) cytosolic Ca^{2+} elevations in response to 20 μM FLA 365 (n=48).

Figure 5. FLA 365 blocks I_{Ba} in canine PASMCs. (A) Ba^{2+} currents over the same time period as cells treated with various Ca_V antagonists. (B) Effects of 10 μM verapamil or (C) 100 μM FLA 365 on I_{Ba}. (D) Bars indicate the percentage of I_{Ba} remaining under time-matched control conditions or in response to 10 μM verapamil or 10 μM or 100 μM FLA 365. Black circles and inset traces show current under control conditions while grey circles and traces show current in response to treatments illustrated in each panel. *** denotes significant difference from control ($P<0.001$) and †† ($P<0.01$) from 10 μM FLA by a one-way ANOVA

with a Newman-Keuls Multiple Comparison Test. Number in parentheses is the number of cells examined. Error bars represent ± SEM.

Figure 6. Ca_V inhibition does not reduce caffeine or 5-HT mediated Ca^{2+} responses in canine PASMCs. (A) Representative tracing of the Ca^{2+} responses to repeated 10 mM caffeine applications. (B) Effects of 10 μM verapamil (Vera) on caffeine mediated Ca^{2+} responses. (C) Effects of 10 μM nifedipine (NIF) on 10 μM 5-HT induced Ca^{2+} responses. (D) Bars indicate the percentage of the $\Delta F_{340}/F_{380}$ relative to an initial application of 10 mM caffeine (solid bars) or 10 μM 5-HT (open bars) in the presence of the agents listed. *** denotes significant difference to other groups treated with caffeine by a one-way ANOVA with a Newman-Keuls Multiple Comparison Test ($P<0.001$). Number in parentheses is the number of cells examined. Error bars represent ± SEM.

Figure 7. FLA 365 reduces 5-HT induced Ca^{2+} responses in canine PASMCs. (A) Representative tracing of the Ca^{2+} responses to repeated 10 μM 5-HT applications. (B) Effects of 2 μM FLA 365 (B) and 20 μM FLA 365 (C) on 10 mM caffeine as well as 10 μM 5-HT elicited Ca^{2+} increases. (D) Bars indicate the percentage of the $\Delta F_{340}/F_{380}$ relative to an initial application of 10 μM 5-HT (solid bars) or 10 mM caffeine (open bars) in the presence of the agents listed. Dashed line represents the height of the Ca^{2+} response due to 10 μM 5-HT prior to FLA 365 application. Significant difference relative to the initial 5-HT stimulation denoted by * ($P<0.05$) and to 10 mM caffeine stimulation in the absence of FLA

365 *** (P<0.01) by a paired t-test. Number in parentheses is the number of cells examined. Error bars represent ± SEM.

Figure 8. FLA 365 blocks carbachol (CCh) elicited Ca^{2+} responses in HEK 293 cells. (A) 2 μM FLA effects on 100 μM CCh induced Ca^{2+} increases. (B) 20 μM FLA effects on 100 μM CCh elicited Ca^{2+} increases. (C) Bars indicate the percentage of the $\Delta F_{340}/F_{380}$ for 100 μM CCh in the absence relative to the presence of the listed agents. (D) Bars show the change in cytosolic [Ca^{2+}] from resting due 100 μM CCh in the absence, presence and following washout of 20 μM FLA 365. Dashed line represents the magnitude of the Ca^{2+} response due to 100 μM CCh prior to FLA 365 application. *** denotes significant difference relative to control by repeated measures ANOVA with a Newman-Keuls Multiple Comparison Test (P<0.001). ††† denotes significant difference between control and 20 μM FLA 365 group by One-way ANOVA with a Newman-Keuls Multiple Comparison Test (P<0.001). Number in parentheses is the number of cells examined. Error bars represent ± SEM.

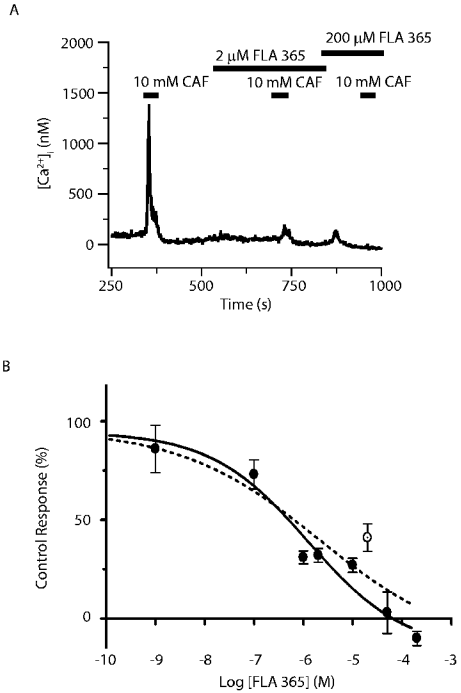
A
200 μM FLA 365
2 μM FLA 365
10 mM CAF
10 mM CAF
10 mM CAF
2000
1500
1000
500
0
[Ca2+]i (nM)
250
500
750
1000
Time (s)
B
100
50
0
Control Response (%)
-10
-9
-8
-7
-6
-5
-4
-3
Log [FLA 365] (M)

Figure 1

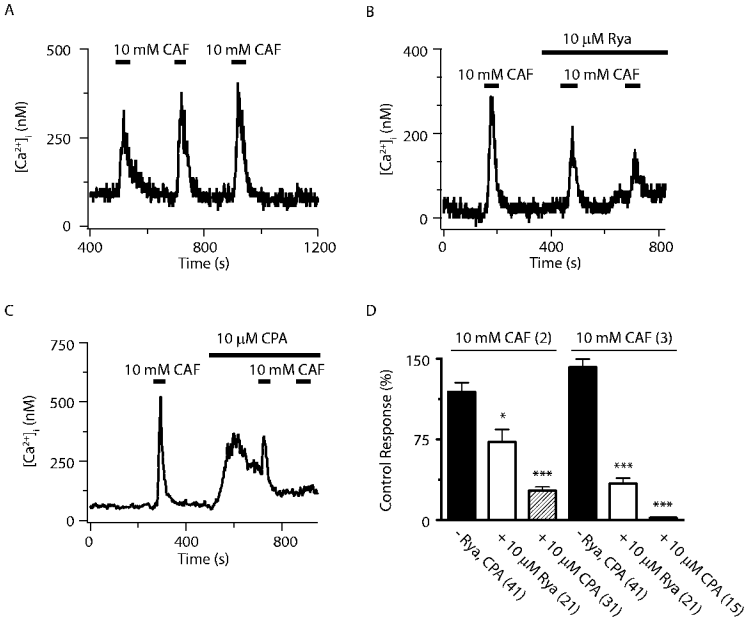
A
500
250
0
[Ca2+]i (nM)
10 mM CAF
10 mM CAF
400
800
1200
Time (s)
B
400
200
0
[Ca2+]i (nM)
10 μM Rya
10 mM CAF
10 mM CAF
0
400
800
Time (s)
C
750
500
250
0
[Ca2+]i (nM)
10 μM CPA
10 mM CAF
10 mM CAF
0
400
800
Time (s)
D
10 mM CAF (2)
10 mM CAF (3)
150
75
0
Control Response (%)
*
***
***
***
-Rya, CPA (41)
+ 10 μM Rya (21)
+ 10 μM CPA (31)
-Rya, CPA (41)
+ 10 μM Rya (21)
+ 10 μM CPA (15)

Figure 2

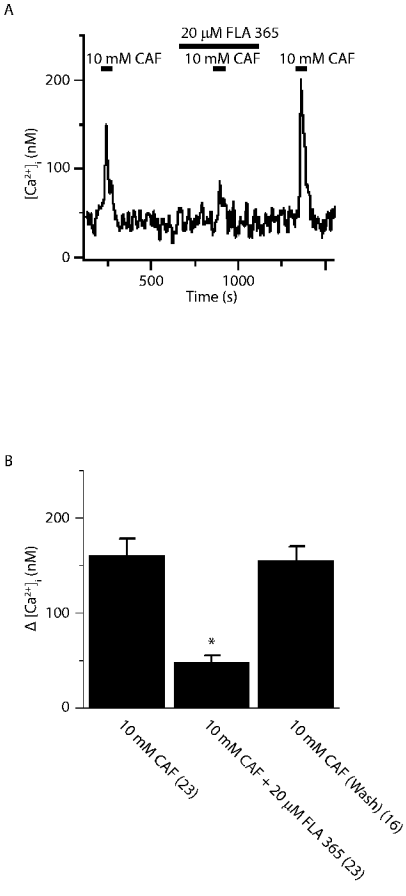
A
20 μM FLA 365
10 mM CAF
10 mM CAF
10 mM CAF
200
100
0
[Ca2+]i (nM)
500
1000
Time (s)
B
200
100
0
Δ [Ca2+]i (nM)
*
10 mM CAF (23)
10 mM CAF + 20 μM FLA 365 (23)
10 mM CAF (Wash) (16)

Figure 3

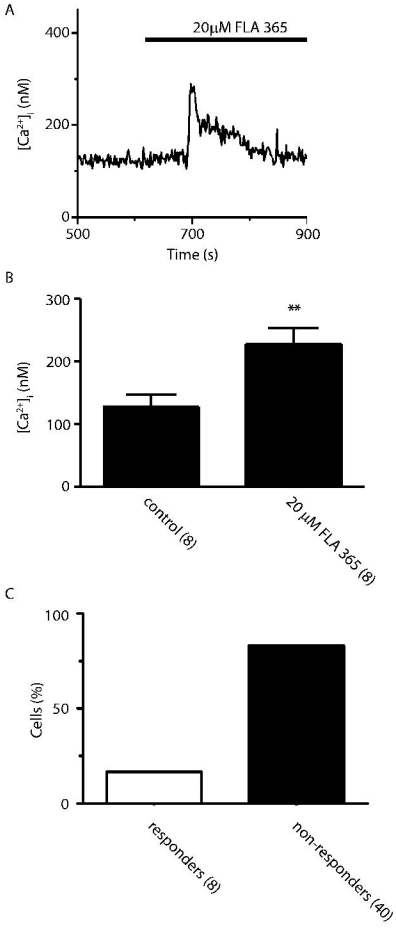
A
20μM FLA 365
400
200
0
[Ca2+]i (nM)
500
700
900
Time (s)
B
300
200
100
0
[Ca2+]i (nM)
**
control (8)
20 μM FLA 365 (8)
C
100
50
0
Cells (%)
responders (8)
non-responders (40)

Figure 4

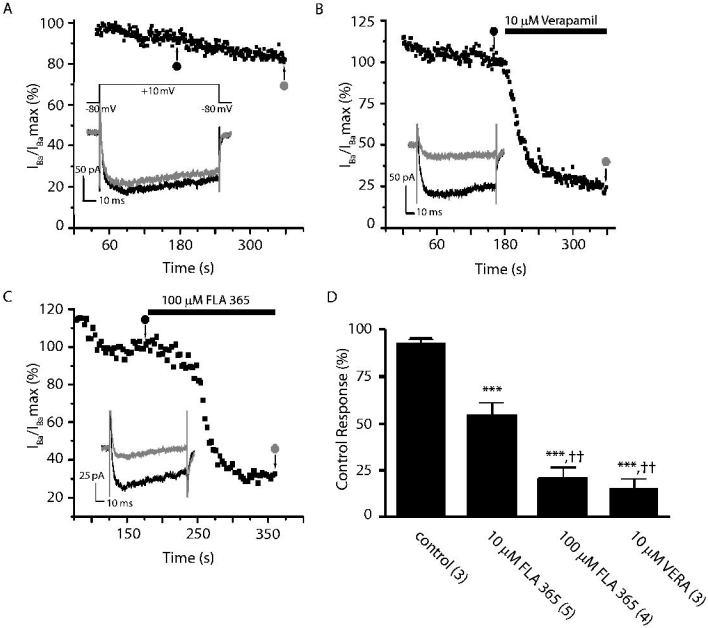
A
B
C
D
+10 mV
-80 mV
-80 mV
50 pA
10 ms
10 μM Verapamil
100 μM FLA 365
25 pA
Time (s)
Control Response (%)
***
***,††
***,††
control (3)
10 μM FLA 365 (5)
100 μM FLA 365 (4)
10 μM VERA (3)

Figure 5

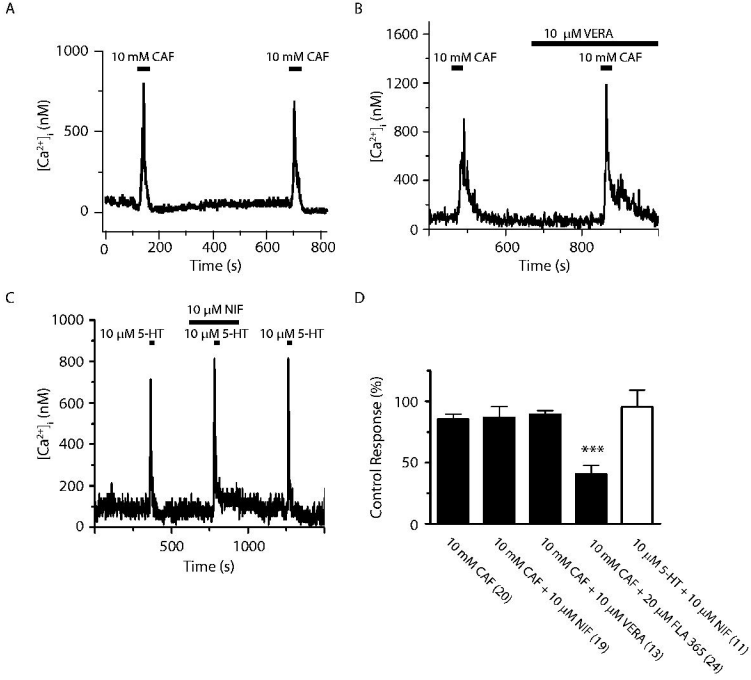
A
10 mM CAF
10 mM CAF
[Ca2+]i (nM)
Time (s)
B
10 μM VERA
10 mM CAF
10 mM CAF
[Ca2+]i (nM)
Time (s)
C
10 μM NIF
10 μM 5-HT
10 μM 5-HT
10 μM 5-HT
[Ca2+]i (nM)
Time (s)
D
Control Response (%)
***
10 mM CAF (20)
10 mM CAF + 10 μM NIF (19)
10 mM CAF + 10 μM VERA (13)
10 mM CAF + 20 μM FLA 365 (24)
10 μM 5-HT + 10 μM NIF (11)

Figure 6

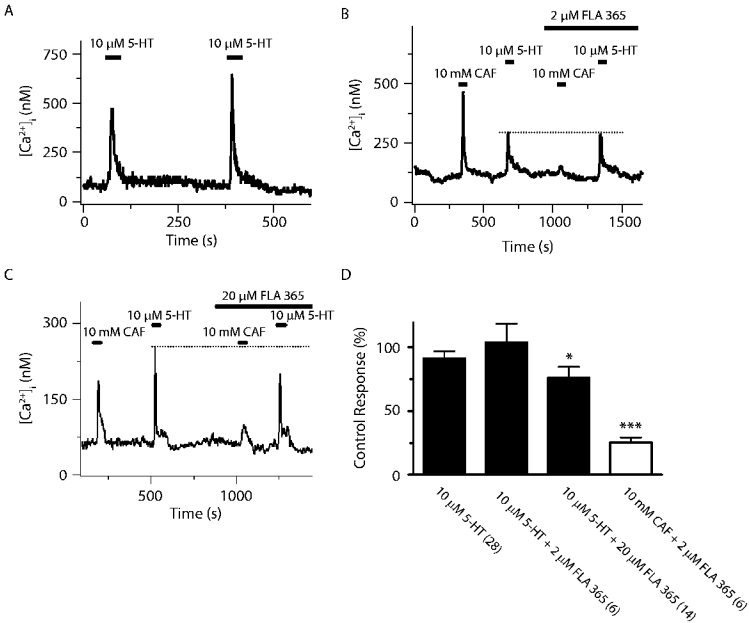
A
10 μM 5-HT
10 μM 5-HT
750
500
250
0
[Ca2+]i (nM)
0
250
500
Time (s)
B
2 μM FLA 365
10 μM 5-HT
10 μM 5-HT
10 mM CAF
10 mM CAF
500
250
0
[Ca2+]i (nM)
0
500
1000
1500
Time (s)
C
20 μM FLA 365
10 μM 5-HT
10 μM 5-HT
10 mM CAF
10 mM CAF
300
150
0
[Ca2+]i (nM)
500
1000
Time (s)
D
100
50
0
Control Response (%)
*
***
10 μM 5-HT (28)
10 μM 5-HT + 2 μM FLA 365 (6)
10 μM 5-HT + 20 μM FLA 365 (14)
10 mM CAF + 2 μM FLA 365 (6)

Figure 7

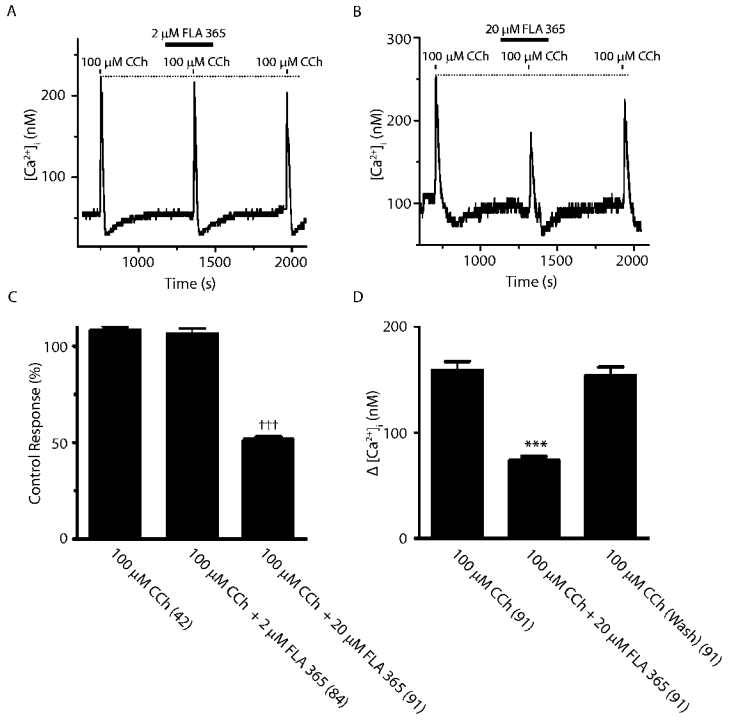
A
2 μM FLA 365
100 μM CCh
100 μM CCh
100 μM CCh
[Ca2+]i (nM)
Time (s)
B
20 μM FLA 365
100 μM CCh
100 μM CCh
100 μM CCh
[Ca2+]i (nM)
Time (s)
C
Control Response (%)
†††
100 μM CCh (42)
100 μM CCh + 2 μM FLA 365 (84)
100 μM CCh + 20 μM FLA 365 (91)
D
Δ [Ca2+]i (nM)
***
100 μM CCh (91)
100 μM CCh + 20 μM FLA 365 (91)
100 μM CCh (Wash) (91)

Figure 8